Journal of Power Sources 226 (2013) 359–362

Contents lists available at SciVerse ScienceDirect

Journal of Power Sources

journal homepage: www.elsevier.com/locate/jpowsour

Short communication

Low-cost porous $Cu_2ZnSnSe_4$ film remarkably superior to noble Pt as counter electrode in quantum dot-sensitized solar cell system

Xianwei Zeng [a], Wenjun Zhang [a], Yan Xie [a], Dehua Xiong [a], Wei Chen [a,*], Xiaobao Xu [a], Mingkui Wang [a,*], Yi-Bing Cheng [a,b]

[a] Michael Grätzel Centre for Mesoscopic Solar Cells, Wuhan National Laboratory for Optoelectronics, Huazhong University of Science and Technology, Wuhan 430074, PR China
[b] Department of Materials Engineering, Monash University, Melbourne, Victoria, 3800, Australia

HIGHLIGHTS

- $Cu_2ZnSnS(Se)_4$ nanoparticles as efficient counter electrodes in quantum dot-sensitized solar cells.
- The catalytic activity is sensitive to the composition and thermal annealing condition.
- Porous $Cu_2ZnSnSe_4$ film sintered at 450 °C at Ar atmosphere was remarkably superior to traditional Pt.
- A high solar conversion efficiency of 4.35% was obtained.

GRAPHICAL ABSTRACT

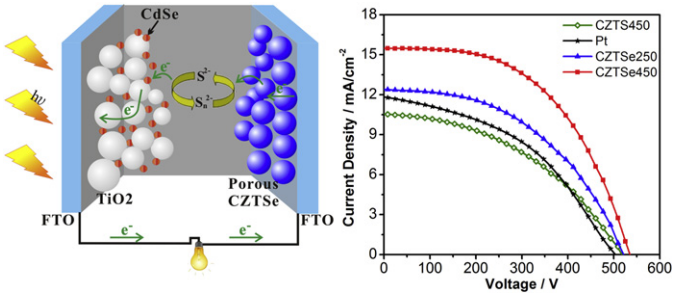

ARTICLE INFO

Article history:
Received 11 August 2012
Received in revised form
20 September 2012
Accepted 9 November 2012
Available online 19 November 2012

Keywords:
Copper zinc tin sulfide
Copper zinc tin selenium
Quantum dot
Solar cells
Counter electrode

ABSTRACT

Lost-cost counter electrodes (CEs) based on $Cu_2ZnSnS(Se)_4$ nanoparticles have been successfully introduced to quantum dot-sensitized solar cells (QDSCs). The investigation has demonstrated that the catalytic activity of $Cu_2ZnSnS(Se)_4$ based CEs is sensitive to the composition and thermal annealing condition. The $Cu_2ZnSnSe_4$ CE with porous structure, fabricated by spray deposition method and sintered at 450 °C in Argon atmosphere, exhibits an excel power conversion efficiency of 4.35% under AM 1.5 solar (100 mW cm^{-2}) irradiation in a QDSC, which is about 70% higher than that of device using the conventional thermally platinized conducting glass CEs.

1. Introduction

Dye-sensitized solar cells (DSCs) have recently been extensively studied as low cost alternatives to conventional inorganic photovoltaic devices. DSC devices showing 12.3% efficiency have recently been achieved by using a judiciously engineered porphyrin sensitizer along with a cosensitizer and a cobalt-based redox shuttle [1]. Though sharing similarity on device configuration as well as photo-to-electricity conversion mechanism, the quantum dot-sensitized solar cell (QDSC) presents much behind photovoltaic performance. Recently, Mn doped CdS/CdSe sensitized solar cell has reached a record of 5.4% power conversion efficiency [2], others being around 4–5% [3]. One of the main limiting factors rests with lack of ideal counter electrode (CE) with high catalytic activity for electrolytes in QDSCs [4]. Platinum (Pt) is now regarded as

* Corresponding authors. Tel./fax: +86 27 8779 3867.
E-mail addresses: wnlochenwei@mail.hust.edu.cn (W. Chen), mingkuiwang@mail.hust.edu.cn (M. Wang).

0378-7753/$ – see front matter © 2012 Elsevier B.V. All rights reserved.
http://dx.doi.org/10.1016/j.jpowsour.2012.11.023

a standard CE material in DSC system [5]; however, it is not efficient for application in QDSC based on polysulfide electrolyte. The adsorption of S^{2-} onto Pt surface decreases the catalysts' surface activity [6]. In order to resolve the problem, alternatives to Pt have been widely exploited, including Au [7], carbon [8], Cu_2S [9], CoS [10], PbS [11], CoS/CuS [6], conducting polymer [12], and Cu_2S/reduced graphene oxide composite [3], etc. Among them, Cu_2S has been demonstrated to be efficient and cost-effective catalyst, and reported frequently in the top category of QDSCs [2,3,9].

Because of the similar *p* type semiconducting property of $Cu_2ZnSnS(Se)_4$ (denoted as CZTS(Se)) to Cu_2S, it is reasonable for us to explore these novel components as CEs in QDSCs. CZTS(Se) are particularly attractive in replacing the widely used $Cu(In,Ga)Se_2$ in thin film solar cells, due to that they have several advantages such as direct band gap with the ideal value of about 1.1–1.5 eV, and importantly can be made of earth abundant elements featuring low-cost and low-toxic [13,14]. Recently, CZTS(Se) have been successfully introduced to DSC system, working as efficient CEs in place of Pt [15].

In this communication, we report on the fabrication of CZTS and CZTSe films by spray deposition of the corresponding nanocrystals, and the application as CEs in QDSC system. Our strategy allows a direct comparison of the associated electrochemical properties between CZTS and CZTSe nanocrystals derived films with various thermal annealing treatments, and investigation on how they affect the device performance. It is interesting to find that, after suitable sintering process, CZTSe based CE exhibits much higher catalytic activity than CZTS and conventional thermally platinized conducting glass CEs towards polysulfide electrolyte.

2. Experimental

CZTS and CZTSe nanocrystals were prepared *via* similar method modified from the literature [14]. Briefly, for CZTS synthesis, 2.0 mmol copper acetylacetonate, 1.5 mmol zinc acetate, 1.0 mmol tin (II) chloride and 4.0 mmol sulphur were added to 40 ml oleylamine and the reaction was kept at 280 °C for 1 h under Ar atmosphere. For CZTSe synthesis, the first part of oleylamine solution (15 ml) containing 4.4 mmol Se, was hot-injected into another part of oleylamine solution (15 ml) containing 1.8 mmol copper acetylacetonate, 1.1 mmol zinc acetate and 0.7 mmol tin (II) chloride. The reaction was taken at 285 °C for 20 min under Ar atmosphere protection.

The as-prepared CZTS and CZTSe nanocrystals dispersed in hexane were sprayed onto FTO glasses (7 Ω square^{-1}, Pilkington, TEC 7) to form homogenous films with controlled thickness of about 600 nm, which were then sintered in a tube furnace under Ar atmosphere at 250 °C or 450 °C for 1 h, used as the CEs (Fig. S1). The thermally platinized FTO glass prepared by pyrolysis of H_2PtCl_6 was used as the reference CE. CdSe quantum dot sensitized TiO_2 film (100 nm dense layer made by spray pyrolysis of titanium diisopropoxide bis(acetylacetonate) + 10 μm thick transparent layer made of 20 nm anatase nanoparticles + 4 μm thick light scattering layer made of 400 nm TiO_2 particles) modified with ZnS was used as the photoanode, prepared by the so-called successive ionic layer adsorption and reaction (SILAR) method according to the literature [9]. QDSCs were made by sandwiching the as-prepared CEs and the photoanodes using Surlyn films (25 μm) as the spacer. The aqueous polysulfide electrolyte containing 1 M Na_2S, 1 M S and 0.1 M NaOH was introduced into the cells *via* vacuum backfilling.

The photocurrent–voltage (*J–V*) characteristics were measured using a Newport AM 1.5G solar simulator (model 91192) at the light intensity of 100 mW cm^{-2}, calibrated by a standard silicon reference cell. The active areas of QDSCs were set at 0.16 cm^2, determined by a square mask. Incident photon-to-current conversion efficiency (*IPCE*) was measured on the basis of a Newport Apex Monochromator illuminator (model 70104). Electrochemical measurements were carried out on a Zahner CIMPS-2 system. For electrochemical impedance spectroscopy (EIS) analysis, the symmetrical cells based on identical CEs (under dark) were set under the potential bias of −0.6 V with the AC amplitude of 10 mV and the testing frequency range was set between 100 mHz and 1 MHz. For Tafel-polarization analysis, the scan rate was set at 50 mV s^{-1}.

3. Results and discussion

The compositions of fresh samples were determined to be $Cu_{2.18}Zn_{0.93}Sn_{0.99}S_{3.90}$, $Cu_{1.95}Zn_{1.18}Sn_{1.03}Se_{3.84}$ by X-ray fluorescence spectroscopy (Fig. S2), very close to the ideal stoichiometric proportion of 2:1:1:4. Fig. 1a–d are scanning electronic microscopy (SEM) images of the as-deposited films sintered at 250 °C and 450 °C for 1 h in Ar atmosphere, which are hereafter denoted as CZTS250, CZTSe250, CZTS450 and CZTSe450, respectively. It is clear that the particle size of CZTS250 film (~10 nm, Fig. 1a) grows evidently after 450 °C thermal annealing (~60 nm for CZTS450 film

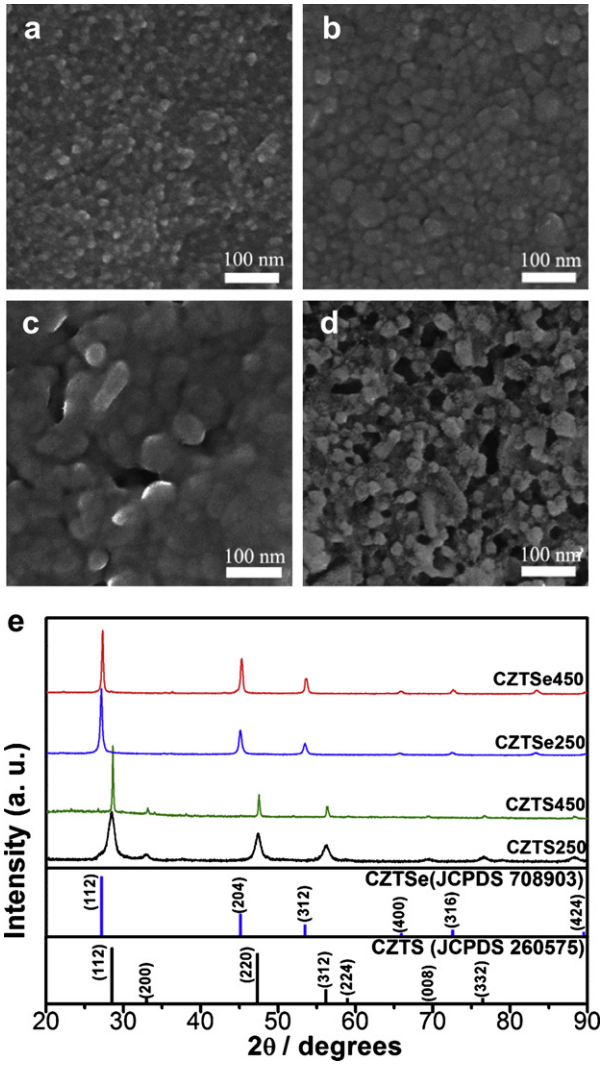

Fig. 1. SEM images of CZTS (a), CZTSe (b) annealed at 250 °C and CZTS (c), CZTSe (d) annealed at 450 °C for 1 h under Argon atmosphere, (e) XRD patterns of the corresponding films.

in Fig. 1c). For CZTSe250 (Fig. 1b) and CZTSe450 (Fig. 1d) films, the particle size nearly keeps constant at ~20 nm and the film morphology changes from densely packed to highly porous. X-ray diffraction (XRD) patterns of the four samples (Fig. 1e) confirm the above mentioned crystal growth associated with thermal annealing. Taking CZTS and CZTSe films for comparison, the thermal stability of CZTSe film seems to be much higher than that of the CZTS film, which could arise from different mass transfer rates of S and Se atoms in the similar kesterite crystal structure. Besides, the porosity of CZTSe450 film is much higher than that of CZTS450 film. The nanosized pore generation is suggested to be derived from the evaporation (or decomposition) of some residual oleylamine molecules which are strongly adsorbed on the surface of CZTSe nanocrystals during the thermal annealing process (as determined by their FTIR spectra in Fig. S3). Less pores leaving in the CZTS450 film should be due to higher degree of crystal fusion during thermal annealing which eliminates the pores.

Fig. 2a shows the *J–V* curves of the QDSCs using CZTS450, CZTSe250, CZTSe450 and Pt as CEs, and the resultant photovoltaic parameters are summarized in Table 1. The device with CZTSe450 CE exhibits an open-circuit photovoltage (V_{oc}) of 0.54 V, a short-circuit photocurrent density (J_{sc}) of 15.49 mA cm^{-2}, and a fill factor (*FF*) of 0.52, giving an overall power conversion efficiency of 4.35%. Compared to the standard device with Pt CE, it is noted that the CZTSe450 CE based QDSC possesses higher efficiency (70.5% improvement in power conversion efficiency), ascribed to much higher J_{sc} (15.49 mA cm^{-2} versus 11.85 mA cm^{-2}), decently higher V_{oc} (0.54 V versus 0.50 V) and *FF* (0.52 versus 0.43) of the former. The overall efficiency of CZTSe250 based QDSC device is the second high among the four tested samples but much lower than the case of CZTSe450. This result reveals the importance of thermal annealing on the catalyst. Furthermore, we studied the influence of components by using S instead of Se. The substitution of Se with S (CZTS450 sample) does not give any improvement in the device photovoltaic performance, due to the low J_{sc} and *FF*. The *IPCE* spectra of the tested cells are shown in Fig. 2b. It is found that *IPCE* maximum of CZTSe450 based QDSC is remarkably higher than others, with a value of 85.3%. Considering the reflectance and absorption losses on FTO glass substrate, the *IPCE* of CZTSe450 based QDSC actually is very close to 100%, indicating that there is nearly no current loss at both the photoanode and CE sides. However, in the case of Pt, CZTSe250 and CZTS450 CEs, the limitation of *FF* and J_{sc} associated with the CEs' catalytic activity is evident. The sequence of *IPCE* for the four tested samples is CZTSe450 > CZTSe250 > Pt > CZTS450, which agrees well with the devices' J_{sc}. This finding indicates that their catalytic activity follows the same tendency. Clearly, the composition variation (replacing S with Se) and thermal post-treatment determine the CZTS(Se) nanoparticles derived films' electrochemical property, and thus, the corresponding QDSCs device photovoltaic performance.

Table 1
Photovoltaic parameters of QDSCs and impedance parameters of the symmetrical cells based on CZTS450, CZTSe250, CZTSe450 and Pt electrodes.

Sample	V_{oc}/V	J_{sc}/mA cm^{-2}	*FF*	η/%	R_s/Ω	R_{ct}/Ω	C_d/μF	Z_w/Ω
Pt	0.50	11.85	0.43	2.55	6.7	68.5	2.1	14.4
CZTS450	0.52	10.53	0.40	2.19	10.2	168.2	1.1	–
CZTSe250	0.52	12.32	0.47	3.01	9.7	16.6	3.8	13.6
CZTSe450	0.54	15.49	0.52	4.35	9.2	8.9	15.4	12.8

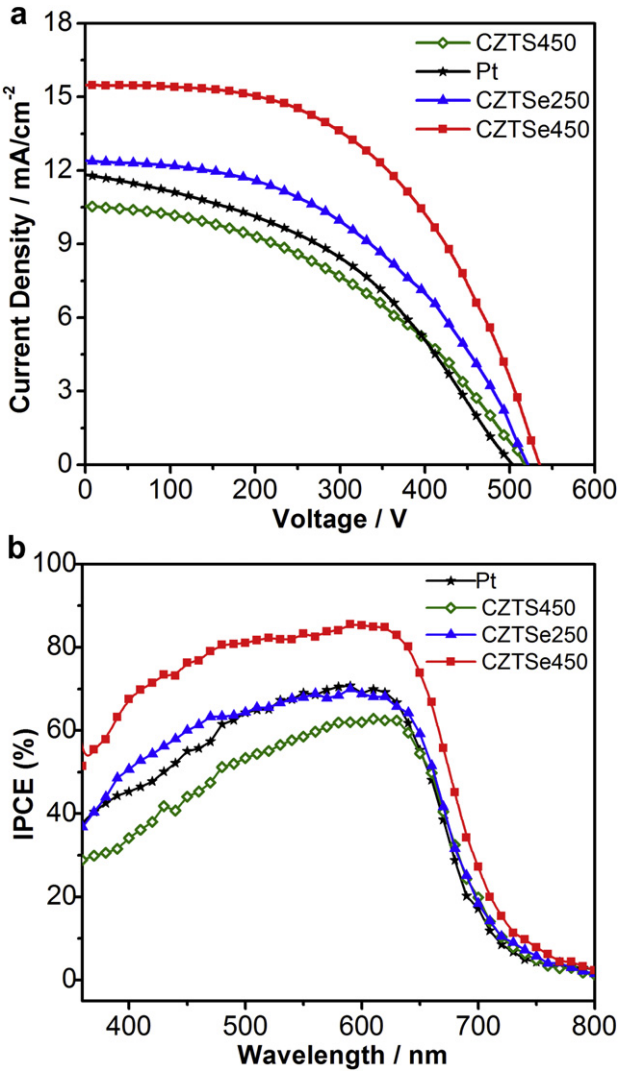

Fig. 2. (a) *J–V* characteristic curves of the QDSCs based on CZTS450, CZTSe250, CZTSe450 and Pt CEs respectively, (b) corresponding *IPCE* spectra of the solar cells.

Fig. 3a shows the EIS results of the symmetrical cells based on the identical CE films, in the form of Nyquist plots. By fitting with a suitable equivalent circuit model shown as the inset in Fig. 3a, the series resistance associated with the catalyst layer covered FTO substrate (R_s), the charge transfer resistance (R_{ct}), the capacitance of electrical double layer (C_d) at the solid–electrolyte interface, and the Warburg diffusion impedance of S_2^{2-}/S^{2-} ions within the electrolyte (Z_w) could be obtained as listed in Table 1. R_{ct} is closely associated with the catalytic activity of different CEs [15]. The smallest value of R_{ct} in the case of CZTSe450 (8.9 Ω) reflects the highest catalytic activity of this material among the four tested samples. R_{ct} of CZTSe450 is found to be about twice lower than that of CZTSe250 (16.6 Ω), reflecting that the importance of sintering temperature to the CZTSe film's catalytic activity. The distinct change on R_{ct} of CZTSe films sintering at a relative high temperature (450 °C) may arise from the following reasons: (1) the elimination of steric hindrance effect caused by the adsorbed oleylamine on CZTSe at an elevated sintering temperature; (2) a sintering induced porous structure of the CZTSe450 film as depicted by SEM images could improve the CZTSe450-electrolye interfacial contact area and therefore increase the possibility for interfacial electron transfer. Larger contact area at the CZTSe450-electrolyte interface is also reflected by its different chemical capacitance [16], C_d = 15.4 μF, evidently larger than that of the other three samples. R_{ct} of CZTS450 (168.2 Ω) and Pt (68.5 Ω) CEs are much larger than that of devices with CZTSe250 (16.6 Ω) and CZTSe450 (8.9 Ω) CEs. R_{ct} also contributes to the total series resistance of the cell which influences

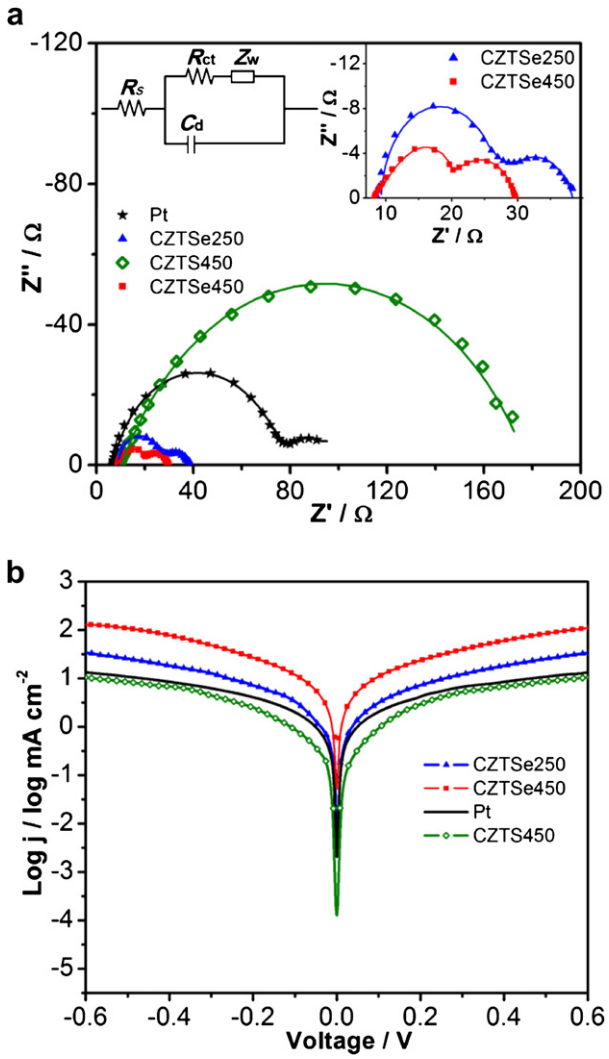

Fig. 3. (a) Nyquist plots and (b) Tafel curves of the symmetrical cells fabricated with identical Pt, CZTS, CZTSe250 and CZTSe450 electrodes. The top-left inset in (a) is the electrical equivalent circuit model used for data fitting.

the *FF*. So, it is reasonable that *FF* of CZTS450 (*FF* = 0.40, R_{ct} = 168.2 Ω) and Pt (*FF* = 0.43, R_{ct} = 68.5 Ω) based QDSCs are smaller than that of CZTSe250 (*FF* = 0.47, R_{ct} = 16.6 Ω) and CZTSe450 (*FF* = 0.52, R_{ct} = 8.9 Ω). The Warburg diffusion resistances (Z_w) for three type of CEs (CZTSe250, CZTSe450, Pt) are nearly the same, implying that no additional limitation from S_2^{2-}/S^{2-} ions diffusion. For CZTS450, the Z_w cannot be identified from its EIS spectrum at the low frequency range.

Fig. 3b presents the Tafel curves of the four different symmetrical cells. In the Tafel zone (in the low bias range), the slopes of the cathodic branches for the four tested samples are in the sequence of CZTSe450 > CZTSe250 > Pt > CZTS450, corresponding to their catalytic activity, respectively. The exchange current density can be evaluated by the equation of $J_0 = RT/nFR_{ct}$ [16], showing that the CZTSe450 has the highest value, much higher than that of the Pt reference. Herein, *R* is the gas constant, *T* being the temperature, *F* being the Faraday constant and *n* being the number of electrons exchanged in the reaction at the electrolyte interface.

4. Conclusions

In summary, porous CZTSe450 film has been demonstrated to work efficiently as CE in QDSC system. Using CdSe quantum dot-sensitized TiO_2 film in combination with the CZTSe450 CE has achieved a power conversion efficiency as high as 4.35%, which can be included in the top category of QDSCs. The improvement in efficiency can be attributed to the high catalytic activity of CZTSe450 CE, partially derived from the nature of CZTSe as well as the porous structure of the film after sintering at relative high temperature. The use of cost-effective CZTSe as alternative to noble Pt, in combination with the easy fabrication method (spray deposition), may promote the possibility on developing low-cost, scalable and highly efficient QDSCs.

Acknowledgements

This work was supported by National Natural Science Foundation (21103058), 973 Program of China (2011CBA00703), Natural Science Foundation of Hubei Province (2011CDB033), the Fundamental Research Funds for the Central Universities (HUST: 2010QN024, 2011TS021).

Appendix A. Supplementary data

Supplementary data related to this article can be found at http://dx.doi.org/10.1016/j.jpowsour.2012.11.023.

References

[1] A. Yella, H.W. Lee, H.N. Tsao, C. Yi, A.K. Chandiran, M.K. Nazeeruddin, E.W.G. Diau, C.Y. Yeh, S.M. Zakeeruddin, M. Gratzel, Science 334 (2011) 629.
[2] P.K. Santra, P.V. Kamat, J. Am. Chem. Soc. 134 (2012) 2508.
[3] J.G. Radich, R. Dwyer, P.V. Kamat, J. Phys. Chem. Lett. 2 (2011) 2453.
[4] S. Ruhle, M. Shalom, A. Zaban, ChemPhysChem 11 (2010) 2290.
[5] H. Bonnemann, G. Khelashvili, S. Behrens, A. Hinsch, K. Skupien, E. Dinjus, J. Cluster Sci. 18 (2006) 141.
[6] Z. Yang, C.Y. Chen, C.W. Liu, C.L. Li, H.T. Chang, Adv. Energy Mater. 1 (2011) 259.
[7] Y.L. Lee, Y.S. Lo, Adv. Funct. Mater. 19 (2009) 604.
[8] Q.X. Zhang, Y.D. Zhang, S.Q. Huang, X.M. Huang, Y.H. Luo, Q.B. Meng, D.M. Li, Electrochem. Commun. 12 (2010) 327.
[9] V. Gonzalez-Pedro, X.Q. Xu, I. Mora-Sero, J. Bisquert, ACS Nano 4 (2010) 5783.
[10] Z. Yang, C.Y. Chen, C.W. Liu, H.T. Chang, Chem. Commun. 46 (2010) 5485.
[11] Z. Tachan, M. Shalom, I. Hod, S. Ruhle, S. Tirosh, A. Zaban, J. Phys. Chem. C 115 (2011) 6162.
[12] M.H. Yeh, C.P. Lee, C.Y. Chou, L.Y. Lin, H.Y. Wei, C.W. Chu, R. Vittal, K.C. Ho, Electrochim. Acta 57 (2011) 277.
[13] Q.J. Guo, H.W. Hillhouse, R. Agrawal, J. Am. Chem. Soc. 131 (2009) 11672.
[14] C. Steinhagen, M.G. Panthani, V. Akhavan, B. Goodfellow, B. Koo, B.A. Korgel, J. Am. Chem. Soc. 131 (2009) 12554.
[15] X.K. Xin, M. He, W. Han, J. Jung, Z.Q. Lin, Angew. Chem. Int. Ed. 50 (2011) 11739.
[16] X. Lin, M.X. Wu, Y.D. Wang, A. Hagfeldt, T.L. Ma, Chem. Commun. 47 (2011) 11489.